Organic & Biomolecular Chemistry

Cite this: *Org. Biomol. Chem.*, 2011, **9**, 2123

www.rsc.org/obc

PAPER

Mechanism and electronic effects in nitrogen ylide-promoted asymmetric aziridination reaction†

Ramanan Rajeev and Raghavan B. Sunoj*

Received 29th October 2010, Accepted 17th December 2010
DOI: 10.1039/c0ob00955e

The mechanism and stereoselectivity of the aziridination reaction between guanidinium ylide and a series of *para*-substituted benzaldehydes have been studied by using density functional theory methods. The mechanistic details and analyses of the key elementary steps involved in (a) the addition of nitrogen ylide to benzaldehydes and (b) subsequent fragmentation of the resulting oxaspirocyclic intermediate are presented. The relative energies of important transition states and intermediates are found to be useful toward rationalizing reported diastereoselective product formation. The relative energies of the key transition states could be rationalized on the basis of the differences in steric, electrostatic, and other stabilizing weak interactions. The deformation analysis of the transition state geometries exhibited good correlation with the predicted activation barriers. The changes in *cis*/*trans* diastereoselectivity preferences upon changes in the electron donating/withdrawing abilities of the *para* substituents on benzaldehyde are identified as arising due to vital differences in the preferred pathways. The large value of reaction constant ($\rho > 4.8$) estimated from the slope of good linear Hammett plots indicated high sensitivity to the electronic nature of substituents on benzaldehyde. The formation of *trans*-aziridine in the case of strong electron donating groups and *cis*-aziridines with weakly electron donating/withdrawing group has been explained by the likely changes in the mechanistic course of the reaction. In general, the predicted trends are found to be in good agreement with the earlier experimental reports.

Introduction

The importance of aziridines has long been recognized owing to their existence as sub-units in many natural products and biologically active molecules.[1] The ability of aziridines to function as enzyme substrates and enzyme inhibitors is known.[2] Highly regio- and stereoselective ring-opening reactions of aziridines have greater value in organic synthesis.[3,4] Azomethine ylides, generated *in situ* from aziridines, can readily undergo [3+2] thermal cycloadditions to furnish pyrrolidine- and pyrrole- containing natural products.[5] While there are several protocols available for the synthesis of structurally diverse aziridines,[6] stereoselective aziridination often poses formidable challenges. The use of chiral auxiliaries[7–9] and chiral catalysts[10–12] has been developed toward realizing enantiopure aziridines.

For the past several decades, ylides have been employed as a source of carbon nucleophiles in a plethora of reactions. Some of the most common examples in this category include the use of phosphorous and sulfur ylides, respectively for Wittig and Corey–Chaykovski reactions.[13] Aggarwal and co-workers offered a series of elegant demonstrations of sulfur ylide promoted epoxidation, cyclopropanation, and aziridination reactions.[14] Selenium ylides also found interesting applications in epoxidation reactions.[15] The sulfur ylide mediated synthesis of aziridines is known to be more effective as a strategy for stereoselective transformations.[16] Control over highly reactive species is often challenging, but such reactants have been put in good use in various reactions. Click chemistry using nitrogen ylides provides a convenient route for the synthesis of structurally diverse nitrogen containing heterocycles.[17] Stereoselectivity in [3+2] addition reactions by using stabilized-, semistabilized-, and nonstabilized-ylides has been well documented in literature.[18]

Although the applications of phosphorous, sulfur, and selenium ylides are widely found in the literature, the number of reports on nitrogen ylides is relatively scarce. The potential of nitrogen ylides appears to be promising in that they could be exploited as a novel class of reagent.[19] In an interesting study, Ishikawa and co-workers demonstrated an efficient method for the synthesis of chiral aziridines by using nitrogen ylides as the chiral auxiliary.[20] They have employed the reaction between guanidinium ylides (henceforth termed as g-ylide in this article) and suitable aryl aldehydes, as shown in Scheme 1, to generate aziridines.[21] More

Department of Chemistry, Indian Institute of Technology Bombay, Powai, Mumbai 400076, India. E-mail: sunoj@chem.iitb.ac.in; Fax: 91-222-576-7152

† Electronic supplementary information (ESI) available: Total energies, optimized Cartesian coordinates of stationary points, additional tables and figures (as mentioned in the text). See DOI: 10.1039/c0ob00955e

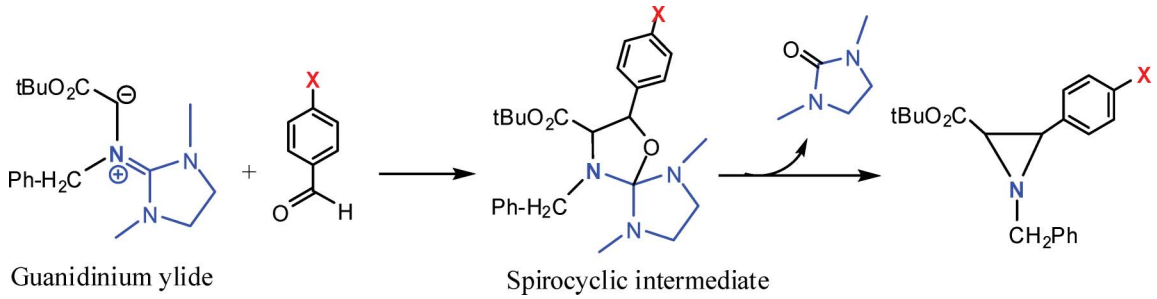

Scheme 1 Aziridine synthesis by using guanidinium ylide.

Table 1 Stereochemical outcome of the aziridination reaction when different EDG or EWG (X) are present at the *para* position of benzaldehyde[a]

Substituent (X)	Classification	Stereoselectivity[b]
O^{n}Bu OMe	Strong EDG	High; *de* > 95, *ee* > 90 of *trans*
CH_3 H	Weak EDG	Moderate; 40–60 *de* and 85–90 *ee* of *cis*
Cl CO_2Me	Weak EWG	Moderate; 40–60 *de* and 80–85 *ee* of *cis*
CN NO_2	Strong EWG	Low; <40 *de* and <30 *ee* of *trans*

[a] The *cis*/*trans* nomenclature is defined with respect to the aryl and ester groups. [b] Ref. 20d.

significantly, it was reported that the introduction of chirality into the guanidinium template could lead to effective asymmetric induction.

One of the very interesting features of Ishikawa's g-ylide promoted asymmetric aziridination reaction is the change in the stereochemical outcome depending on the nature of the electrophile. The diastereoselectivities are found to be dependent on the presence of an electron donating (EDG) or withdrawing (EWG) group at the *para* position of benzaldehyde.[20d] Selected examples illustrating the effect of substituents (X) on the stereochemical outcome of the reaction are grouped together in Table 1. This observation readily invites a detailed study of the contributing stereoelectronic factors.

The product distribution and the stereochemical outcome in these reactions could depend on the availability of π-electrons, and geometric dispositions as well as the nature of substituents near the reaction site. Improved understanding on stereoselectivity can be developed by a detailed analysis of electronic, steric, and weak interactions operating in the crucial transition states involved in various elementary steps of the reaction.[22] Fine-tuning of these factors could help design new chiral catalysts/auxiliaries for a better outcome.[23]

Considering the underlying potential of nitrogen ylide chemistry, and in view of the interesting stereochemical course of aziridination reactions, we have undertaken a detailed examination of the mechanism of guanidinium ylide promoted aziridine formation. Besides analyzing the energies and geometries of the key intermediates and transition states, linear free energy relationships (by considering a series of electrophiles), have also been examined in the present study.[24] The correlation between the computed activation energies and distortion of electrophilic and nucleophilic fragments are also studied.[25]

Computational methods

All the calculations were carried out by using Gaussian03 suite of quantum chemical programs.[26] Three popular density functional theory methods were employed in this study. These include mPW1K, mPW1PW91, and B3LYP functional. The primarily choice of functional has been the hybrid density functional mPW1K for the present study.[27] Additional computations by using B3LYP[28] and mPWPW91 functionals were also performed.[29] Pople's basis set 6-31G* was used for all calculations. All transition states were fully optimized and characterized as first-order saddle point by harmonic vibrational frequency analysis. The one and only one imaginary frequency of the first-order saddle point was first subjected to visual inspection to examine whether it represents the desired reaction coordinate in each case. Further verifications of the transition states were carried out by using the intrinsic reaction coordinate (IRC) calculations.[30]

The effect of continuum solvation was incorporated by using the polarizable continuum model (PCM).[31] Since the available experimental reports employed tetrahydrofuran (THF) as the solvent, we have chosen the dielectric constant of THF (ε = 7.58) for calculations in the condensed-phase. Additional energy refinements within the PCM formalism were carried out by using a more flexible basis set at the mPW1K/6-311++G** level of theory. This energy in solution is comprised of the electronic energy of the polarized solute, electrostatic solute–solvent interaction energy, and nonelectrostatic terms corresponding to cavitation, dispersion, and short-range repulsion.

Results and discussion

As discussed in the introduction, the product distribution exhibits an interesting sensitivity to the nature of the *para*-substituent attached to the electrophilic benzaldehyde. It is therefore inherently interesting to provide a rational framework to understand the controlling factors that influence the stereoselectivity in g-ylide promoted aziridination. A number of key details, such as the knowledge of the reaction mechanism and the nature of energy profile should be taken into account to achieve this objective. The mechanism of g-ylide catalyzed aziridination is suggested to involve two key steps, *viz*., addition and fragmentation, as shown in Scheme 2. The addition step consists of the C–C bond formation between the g-ylide and aryl aldehyde. The zwitterionic species thus produced can quickly cyclize to a spirocyclic intermediate.[32]

The discussions are broadly grouped into two major sections; (I) the addition of g-ylide to aldehyde leading to the formation of

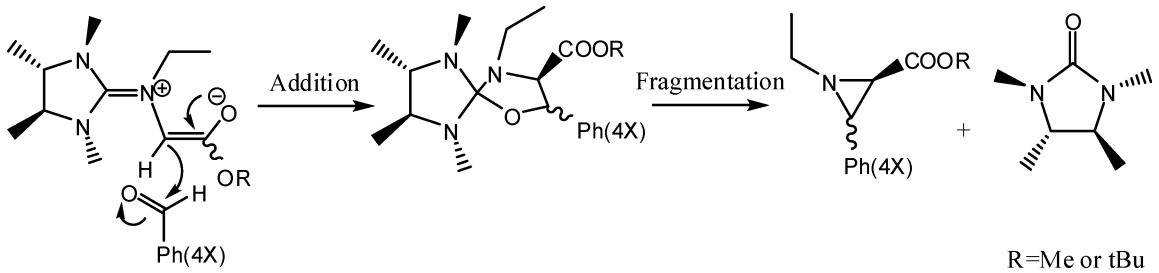

Scheme 2 The key steps involved in the mechanism of aziridination using guanidinium ylides. A representative example for the addition of *re* face of g-ylide to the *re* face of aryl aldehyde is shown.

an oxa-spirocyclic intermediate, and (II) the fragmentation of the oxa-spirocyclic intermediate (1-oxa-4,6,9-triazaspiro[4.4]nonane) to aziridine. Benzaldehydes with a range of *para* substituents (X), from strong electron withdrawing to strong electron donating groups, are considered as electrophiles. Two model systems for nucleophiles, differing in terms of the ester R group (R = *tert*-butyl or Me), as shown in Scheme 2, are examined.

(I) Addition of g-ylide to aldehyde

In the first step, four stereochemically distinct possibilities for the C–C bond-formation are considered between g-ylide and aldehyde. The g-ylide can approach either the *si* or *re* face of the aldehyde, through two of its prochiral faces. The transition states (TS) for all these possibilities are located to account for the stereoselectivity induced in the first step of the reaction. It is of significance to note that the *cis* or *trans* stereochemistry of aziridine would primarily be decided by the mode of approach between the prochiral faces of g-ylide and the electrophile. For example, the addition of *re* face of g-ylide on the *re* face of aldehyde (*re–re* mode) leads to a *trans* oxa-spirocyclic intermediate.[33] The stereochemistry of the final product would continue to remain *trans* if the ensuing fragmentation proceeds through an S_Ni-like pathway. However, ring opening of the oxa-spirocyclic intermediate, followed by an S_N2-like pathway would lead to a 2,3-*cis*-aziridine (*vide infra*). Conformations of g-ylide have been chosen by keeping the bulkier groups as far away as possible so as to minimize potential unfavorable interactions. For this, the imidazolidine ring and the *tert*-butyl carboxylate groups should remain away from each other. These conformations were retained in subsequent fragmentation step as well.

The computed relative energies of TSs with respect to the most preferred mode for the addition step are provided in Table 2. Of the four key stereochemical modes, it is evident that the *re–re* mode is energetically the most preferred at the $PCM_{(THF)}$/mPW1K/6-311++G**//6-31G* level of theory. The trend is found to be the same at other levels of theory such as the B3LYP and mPW1PW91 as well.[34] Interestingly, the *re–re* mode of addition consistently remains as the most preferred approach, irrespective of the nature of the *para* substituent on benzaldehyde. This observation indicates that the stereochemical outcome, if it stems from the addition step, would be a result of the *re–re* mode of addition. High enantioselectivity, as noticed in the reported experimental results, can be explained by comparing the energies of $TS1_{re–re}$(H) with that of $TS3_{si–si}$(H) in the case of benzaldehyde.

Table 2 Relative energies (in kcal mol^{-1}) of transition states for the addition of g-ylide to benzaldehyde with various substituents (X) at the *para* position obtained at the $PCM_{(THF)}$/mPW1K/6-311++G**//mPW1K/6-31G* level of theory[a]

X[b]	$TS1_{re–re}$	$TS2_{re–si}$	$TS3_{si–si}$	$TS4_{si–re}$
CN	0.00	–0.07	5.76	5.58
COOMe	0.00	1.37	5.45	5.45
Cl	0.00	1.28	5.44	5.14
H	0.00	1.64	4.89	4.73
Me	0.00	1.63	4.73	4.52
OMe	0.00	1.22	4.61	4.18
OH	0.00	1.24	4.50	4.27

[a] For each substituent, the relative energy is calculated with respect to the lowest energy transition state. [b] Transition state, $TS1_{re–re}(NO_2)$ could not be successfully optimized, as all attempts led to a saddle point with low imaginary frequency not pertaining to the reaction coordinate.

A representative set of TS geometries for the addition of g-ylide to benzaldehyde is provided in Fig. 1. The developing C–C bond distance (reaction coordinate) indicates relatively tighter TSs for both *re–re* and *re–si* modes of addition. The predicted energy differences between the C–C bond formation TSs are found to exhibit a reasonable dependence on the relative dispositions of the phenyl group of benzaldehyde and the carboxylate ester and guanidinium group of g-ylide. For instance, in $TS1_{re–re}$(H), the benzaldehyde phenyl group occupies a sterically less demanding position as compared to that in $TS2_{re–si}$(H). The key dihedral angle, C1–C2–C3–C4 for $TS1_{re–re}$(H) and $TS2_{re–si}$(H) are respectively found to be −71° and 43°.[35] In $TS2_{re–si}$(H) on the other hand, the phenyl group remains at a bisecting position of the C1–C2–N1 angle, causing slightly higher steric interaction with the ester group. A potential destabilizing Coulombic interaction between the lone pairs on oxygen and the phenyl ring in $TS2_{re–si}$(H) is likely. Another weakly stabilizing C–H $\cdots\pi$ interaction between the phenyl group and *tert*-butyl group of g-ylide is identified in $TS1_{re–re}$(H).[36] The AIM analyses could identify a bond path consisting of a bond critical point (ρ_{bcp} = 0.003) between the phenyl ring and one of the *tert*-butyl hydrogen atoms in this TS. The *si*-face of g-ylide being relatively more hindered, the electrophile will experience higher steric interaction in the *si–si* mode of addition. It is important to note the orientation of the nitrogen substituent in $TS3_{si–si}$(H). The ethyl group attached to N1 appears to be conformationally restricted due to the interactions with the N-methyl groups of the imidazolidine ring. The ethyl group therefore is pointed towards the *si* face of g-ylide. In fact, the introduction of a benzyl group on N1 has been examined

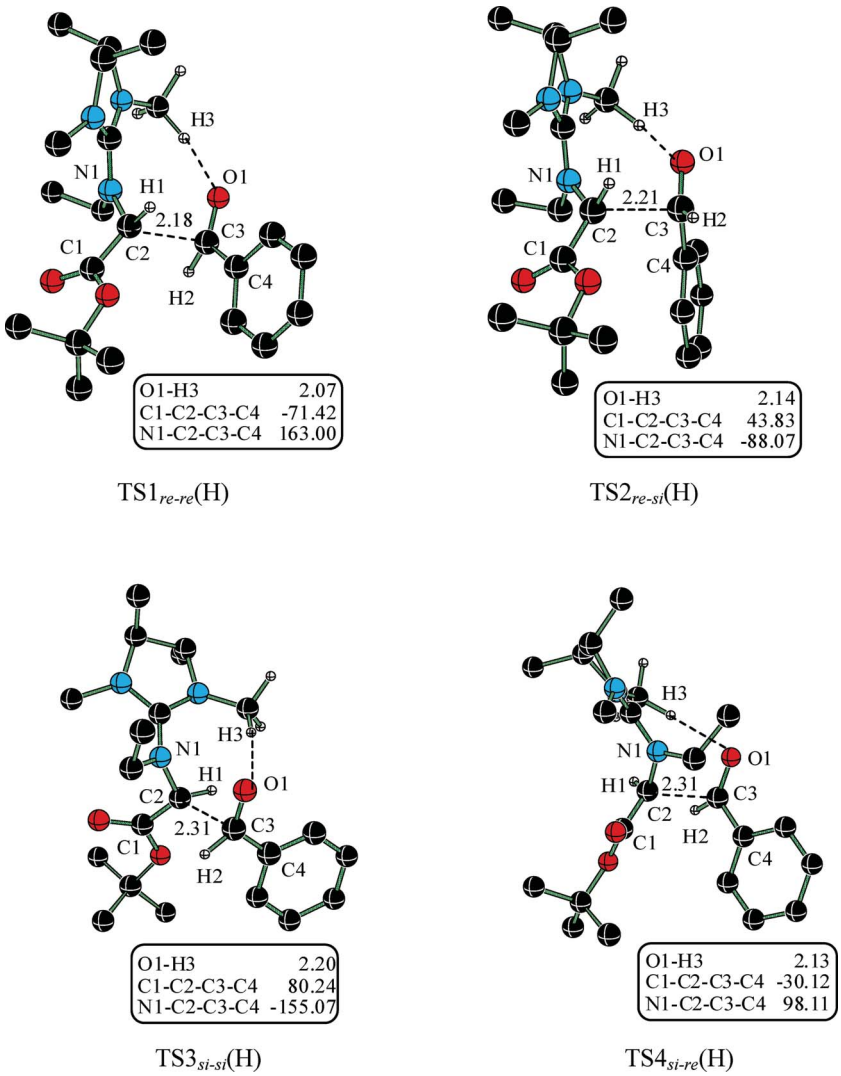

Fig. 1 The mPW1K/6-31G* optimized transition state geometries for stereochemically distinct modes of addition of g-ylide to benzaldehyde TS(H).

in an earlier experimental study. The insights of this level could help design newer g-ylide promoters for asymmetric aziridination reactions. The cumulative effect of the above-mentioned steric as well as other weak interactions is found to be effective in rationalizing the relative energy order between different TSs. The steric interactions are further identified to have a direct bearing on whether the TSs are tightly held or loosely bound. For both the TSs, where the crowded *si* face of g-ylide is involved in the addition, a longer C2–C3 incipient distance is evident (2.31 Å for both $TS3_{si-si}$(H) and $TS4_{si-re}$(H)).

As highlighted earlier with the help of Table 1, the *cis*/*trans* diastereoselectivity in aziridination delicately depends on the ability of the *para* substituents to act as an electron withdrawing or electron donating group. Besides the steric control offered by the guanidinium group, other latent electronic factors could influence the stereochemical outcome. To gain improved insights on the role of substituents and their effect on the computed activation barriers, the extent of deformation accompanying the addition of g-ylide on aldehydes is examined. Since the incoming nucleophile remains the same, the correlation between the deformation energy and the computed activation barriers could be regarded as arising primarily due to the electronic features of the aldehydic acceptor. The degree of pyramidalization (DOP) of the aldehydic carbonyl carbon is taken as the key deformation coordinate. The analysis is further extended to the ylidic carbon that adds to the electrophile. Such deformation analyses have been commonly employed toward explaining the reactivity-selectivity principle in cycloaddition as well as other reactions.[25] The degree of pyramidalization (DOP) around these two carbon atoms at the TSs can be regarded as a direct measure of the extent of deformation associated with a trigonal to tetrahedral conversion due to the C–C bond formation. The magnitudes of computed DOP are provided in Table 3.

The analysis of the changes in the reactant geometries from the initial trigonal planar to tetrahedral-like arrangement upon going from reactant to transition states, on the basis of the data provided in Table 3, clearly conveys that the relative energies of the transition states are directly proportional to the extent of deformation. The DOP of the carbonyl carbon of aryl aldehydes, in the *re–re* and *re–si* modes, exhibits a steady increase upon changing the *para* substituent from strong electron withdrawing to strong electron donating. Similar effects are also noticed for the ylidic carbon atom involved in the C–C bond formation. For instance, the

Table 3 Degree of pyramidalization (in °) around the carbonyl carbon of electrophile (A) and the carbon atom of ylide (G)[a] computed at the mPW1K/6-31G* level of theory

	$TS1_{re–re}$		$TS2_{re–si}$		$TS3_{si–si}$		$TS4_{si–re}$	
Substituent (X)	G	A	G	A	G	A	G	A
NO_2	[b]	[b]	15.1	4.2	11.3	1.5	12.3	1.7
CN	12.5	3.2	15.8	4.7	12.9	1.9	13.8	2.1
COOMe	14.2	4.5	15.1	4.3	14.6	2.5	15.5	2.6
Cl	15.2	5.4	15.9	4.9	15.8	3.1	17.2	3.3
H	15.6	5.7	16.0	5.0	16.9	3.7	18.6	4.0
Me	15.9	5.9	16.5	5.5	17.3	3.8	18.9	4.2
OMe	16.6	6.6	17.1	6.0	18.1	4.3	20.1	4.8
OH	16.3	6.3	17.0	6.0	18.0	4.2	19.5	4.6

[a] DOP in the TS geometry is calculated as the difference between the sum of angles subtended by all three substituents attached to the carbonyl carbon and that of a fully planar situation (360°). [b] Transition state, $TS1_{re–re}(NO_2)$ could not be successfully optimized, as all attempts led to a saddle point with an undesirable low imaginary frequency.

DOP at the aldehydic and ylidic carbon atoms for $TS1_{re–re}$(CN) is respectively 3.2° and 12.5°, whereas the corresponding values for $TS1_{re–re}$(OH) are 6.3° and 16.3°.[37] Furthermore, interesting trends in distortions are noticed within a given series, depending upon the stereochemical mode of addition. As expected, when the electrophile approaches the sterically more crowded *si*-face of g-ylide, the DOP is found to be larger. The deformations at the g-ylide are in line with the increase in the relative energies of the corresponding TSs in the same series. This can be readily examined by inspecting the DOP of the ylidic carbon in the reaction between g-ylide and benzaldehyde. The DOP in $TS1_{re–re}$(H) is 15.6° which shows a progressive increase to 18.6° in $TS2_{si–re}$(H). Interestingly, the DOP at the aldehydic carbon atom shows an inverse trend along the same series. For the most preferred $TS1_{re–re}$(H) the DOP is 5.7, whereas it is 4.0 for the highest energy $TS2_{si–re}$(H). In summary, the effect of deformation of nucleophilic g-ylide appears to have a more pronounced effect on the overall barrier as compared to the corresponding effect noticed with the aldehydic carbonyl group. The deformation energies of the incoming nucleophile and electrophile are further examined by using the activation-strain model popularized by Bickelhaupt. These energies are calculated by comparing the energies of both nucleophile and electrophile in the same geometries as noticed with the respective pre-reacting complexes and the corresponding TSs. The trends of DOP and deformation energies are found to be similar.[38]

(I.a) The Hammett correlations in the C–C bond formation step. The activation barriers for the addition of g-ylide on aryl aldehydes, computed with respect to the corresponding pre-reacting complexes (PRC), are provided in Table 4. These PRCs are traced by using careful geometry optimization starting from the last point of the IRC runs.[39] The PRCs are further verified as true minima on the respective potential energy surfaces by evaluating the corresponding Hessian indices. It is evident from the computed barriers that strong electron withdrawing groups tend to lower the activation barriers. For instance, *para*-nitrobenzaldehyde exhibits the lowest barrier, whereas *para*-methoxy- or *para*-hydroxy- benzaldehydes are relatively on the higher side in the present series. Such changes are evidently due to the subtle variations in the electrophilic character of the carbonyl carbon due to changes in the nature of substituent at the *para* position. This trend further alludes to a possibility that the rate-determining step could change depending on the nature of the electron donating or withdrawing abilities of the *para* substituent. While the initial addition step is likely to be rate-controlling with strong electron donating groups, any of the subsequent steps might well become rate-controlling in the case of strong electron withdrawing substituent.

Table 4 Gibbs free energy of activation (in kcal mol^{-1}) obtained at the mPW1K/6-31G* level of theory for the addition of g-ylide on aryl aldehydes bearing various substituents at the *para* Position[a]

Substituent (X)	$TS1_{re–re}$	$TS2_{re–si}$	$TS3_{si–si}$	$TS4_{si–re}$
NO_2	[b]	3.56	10.43	10.75
CN	3.93	6.07	10.66	11.17
COOMe	4.94	6.77	12.22	12.73
Cl	6.50	7.75	12.96	13.23
H	7.22	8.47	14.06	13.95
Me	8.04	9.68	15.26	15.34
OMe	8.83	10.14	15.39	16.04
OH	8.83	10.34	15.45	15.54

[a] Absolute energies are with respect to the corresponding PRCs. [b] Transition state, $TS1_{re–re}(NO_2)$ could not be successfully optimized, as all attempts led to a saddle point with low imaginary frequency not pertaining to the desired reaction coordinate.

The variations in the electronic effects at the reaction site arising due to the changes in the nature of the *para* substituents and the corresponding changes in the activation barriers for the addition step is further probed with the help of Hammett correlations.[40] The kinetic quantities such as the free energies of activation for the substituted and unsubstituted benzaldehydes, in the form of $-(\Delta G^{\ddagger}_{x} - \Delta G^{\ddagger}_{H})$, are plotted against Hammett constants (σ_x) (Fig. 2).[41] Impressive linear correlations are noticed for *re–re* and *si–si* modes of addition between g-ylide and benzaldehyde.[42] The Hammett linear correlations evidently reveal positive slopes (ρ) for all modes of addition, conveying that an accumulation of negative charge is taking place at the transition states. This observation is in concurrence with the mechanism considered in this study that it involves the addition of g-ylide on aldehyde, leading to the development of an alkoxide ion. Another interesting observation arising from this analysis is a large value of reaction constant ρ, implying that the barrier for the addition of g-ylide is sensitive to the nature of the substituent X on benzaldehyde. The Hammett correlations suggest that the reaction might show critical variations depending on the nature of the substituent.

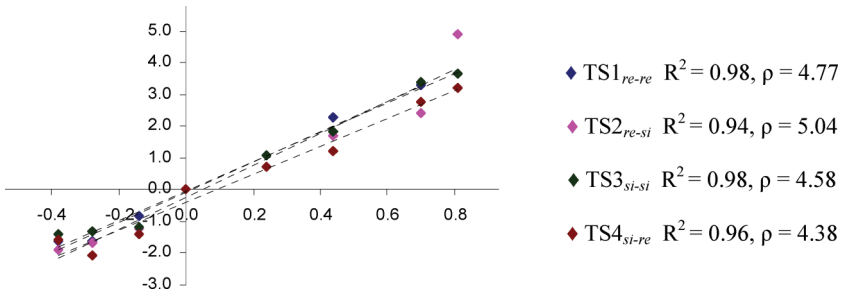

Fig. 2 Hammett plots for the four stereochemical modes of addition of g-ylide (R = *tert*-butyl) to *para*-substituted benzaldehydes. The Y- and X-axes are respectively $-(\Delta G^{\ddagger}_{x} - \Delta G^{\ddagger}_{H})$ and substituent constant (σ_x).

Although the general trends emerging through the analysis of the relative energies of the TSs for the addition step is in favor of *trans* aziridine, the formation of *cis* aziridines is reported as the major product in the case of aryl aldehydes bearing a weakly electron donating group. This observation suggests that the mechanistic course after the addition step, could equally be significant toward the overall stereochemical outcome of this reaction. The relative orientations of C2 and C3 substituents in the most preferred *re–re* mode of addition suggest that a *trans* oxa-spirocyclic intermediate would be the major product in the first step, which can eventually lead to *trans* aziridine. In view of this, ensuing steps responsible for the collapse of the oxa-spirocyclic intermediate are examined next.

(II). Fragmentation of the oxa-spirocyclic intermediate

The fragmentation of the oxa-spirocyclic intermediate can proceed by two key pathways. The first possibility involves the attack of the nitrogen on the benzylic carbon leading to the formation of aziridine, as shown in Scheme 3. The mechanism is similar to an internal nucleophilic substitution S_Ni, wherein the stereochemistry of the product is retained as that in the oxa-spirocylic intermediates.

The second possibility, as shown in Scheme 4, involves the ring-opening of oxazolidine through a rotation around the C2–C3 bond, followed by a nucleophilic substitution at the benzyl carbon. The attack of the internal nucleophilic nitrogen on the benzylic carbon facilitates the release of imidazolidinone besides generating the desired aziridine. Such an S_N2-like mechanism can result in inversion of stereochemistry at the benzylic carbon.

As discussed earlier, the activation barriers for the initial addition step increase with the electron donating ability of the *para*-substituent. Higher barriers for strong EDG underscore the importance of the addition step in stereoselectivity. The major product is identified as the *trans* isomer in the case of a strong EDG. Furthermore, the predicted trend is in concurrence with the reported slower reaction rate for strong EDG.[23d] The energetic comparison between various TSs involved in S_Ni and S_N2 pathways are provided in Table 5. The TSs for the fragmentation through S_Ni-like pathway for the *trans* and *cis* isomers of oxa-spirocylic intermediate are respectively denoted as $TSf1_{trans}$ and $TSf2_{cis}$. The rotational transition states, involved in the alternative pathway are designated as $TSr_{cis/trans}$, depending on the relative configuration of the substituents on the oxa-spirocyclic intermediate. The S_N2 pathway proceeds either through TSf3 or TSf4. The relative energies evidently show that the S_Ni-like TSs are much higher in energy. For instance, in the case of benzaldehyde the relative energies of $TSf1_{trans}$ and $TSf2_{cis}$ are respectively 40.2 and 47.6 kcal mol^{-1} with respect to the separated reactants. The relative energies of rotational TSs, on the other hand, are found to be 28.4 and 36.8 kcal mol^{-1} respectively for TSr_{trans} and TSr_{cis}. Evidently, the S_N2-like pathway is more preferred which would result in a rotation around the C2–C3 bond. In general, the ring opening of *trans*-oxa-spirocyclic intermediate appears to be more favorable than the corresponding *cis* isomer. Furthermore, an EWG tends to favor the ring opening process more than an EDG within a given

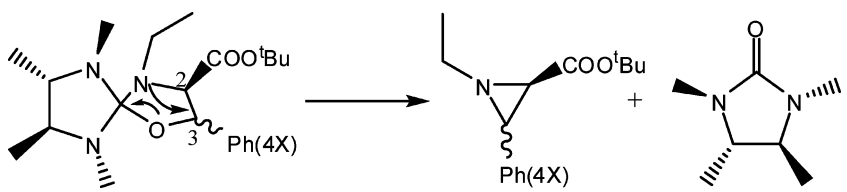

Scheme 3 The formation of aziridine through S_Ni like fragmentation of the oxa-spirocyclic intermediate.

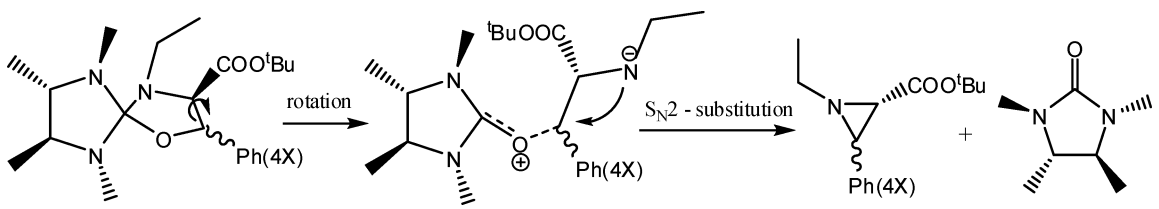

Scheme 4 The formation of aziridine through S_N2-like fragmentation of the oxa-spirocyclic intermediate.

Table 5 Relative energies (in kcal mol^{-1}) of key transition states computed at the PCM$_{(THF)}$/mPW1K/6-311++G**//mPW1K/6-31G* level of theory for aziridination reaction from the oxa-spirocyclic intermediate

X	TSf1$_{trans}$	TSf2$_{cis}$	TSr$_{trans}$	TSr$_{cis}$	TSf3	TSf4
NO_2	40.48	44.84	25.64	31.59	30.13	23.62
CN	40.93	45.64	25.98	32.71	30.79	24.70
COOMe	39.37	46.60	27.04	34.29	32.70	26.18
Cl	42.09	47.01	28.03	35.26	33.01	27.43
H	40.22	47.59	28.44	36.78	33.74	28.76
Me	40.58	47.75	29.43	39.01	34.81	29.61
OMe	40.43	42.31[a]	31.09	38.75	35.51	30.37
OH	40.33	42.15[a]	30.92	38.50	[b]	30.82

[a] TSs are optimized at the mPW1K/6-31G* level of theory with constraints on dihedral angle around the C2–C3 bond, as attempts with full degree of freedom resulted in undesired products. [b] TS could not be optimized at the mPW1K/6-31G* level of theory.

configuration. The competitive pathways for *cis* and *trans* aziridine formation can be regarded as (i) *cis*-oxa-spirocyclic intermediateas → TSr$_{cis}$ → TSf4 → *trans*-aziridine, and (ii) *trans*-oxa-spirocyclic intermediateas → TSr$_{trans}$ → TSf3 → *cis*-aziridine. Another interesting feature due to the changes in the nature substituents on benzaldehyde relates to the diminishingly smaller differences between the energies of TSr$_{cis}$ and TSf3, when a strong EWG such as -NO_2 is introduced. For instance, the energy difference between TSf3-(NO_2) and TSr$_{cis}$-(NO_2) for *para*-nitrobenzaldehyde is found to be 1.45 kcal mol^{-1}, as compared to the corresponding difference of 3.04 kcal mol^{-1} in the case of benzaldehyde. This can be attributed to the destabilizing effect in the S_N2-like TS caused by the EWG. The charge stabilization in the crucial intermediates and TSs can exert a pivotal effect on the mechanistic course of the reaction. The developing partial positive charge on the benzylic carbon can benefit from the stabilization offered by the EDG while it would result in destabilization when a strong EWG (X = NO_2, CN) is attached. The diminishing energy difference between TSf3 and TSr$_{cis}$ in the two competitive pathways for a strong EWG is a clear indication that the substituents can alter the diastereoselectivity in favor of *trans*-aziridine.

The reported *cis* selectivity for weak EDG as well as weak EWG groups (X = COOMe, Cl, H, Me) is in agreement with the relative energies of rotational transition states. The *cis* selectivity can be explained by comparing the energies of the rotational transition states.[45] Since the energy of rotational TSr$_{trans}$ for *trans*-spirocyclic intermediate is lower than that for the corresponding *cis* intermediate TSr$_{cis}$, the rotation of *trans* isomer followed by an S_N2 step can lead to *cis*-aziridine as the major product. While the relative energies of TSs for direct fragmentation of the oxa-spirocyclic intermediate are higher, additional stabilization through the likely participation of additives, such as acetic anhydride, under the experimental conditions might facilitate an S_Ni-like pathway.[43]

Interesting geometric features capturing the above-mentioned energy order between TSs became evident through careful analysis. A representative set of TS geometries for S_Ni like fragmentation step is provided in Fig. 3. The position of the N-ethyl group is identified as important as it can develop repulsive interactions with the imidazoline methyl groups. This interaction is found to be different in the fragmentation TSs for *trans* and *cis* spirocyclic intermediates. This insight could be vital toward considering suitable substituents on the nitrogen of g-ylide. In TSf2$_{cis}$ the N-ethyl and C3 phenyl groups are in a *cis* disposition while they remain far separated in TSf1$_{trans}$. This geometric feature can be gleaned from N1–C2–C3–C4 dihedral angles, which are 163.6° and −54.3° respectively in TSf1$_{trans}$ and TSf2$_{cis}$.

The optimized TS geometries for the second possibility, wherein the oxa-spirocyclic intermediate undergoes a rotation around the C2–C3 bond, instead of a direct S_Ni-like ring closure, is given in Fig. 4. For *cis* and *trans* oxa-spirocyclic intermediates, the bulkier *tert*-butyl carboxylate and imidazolidine groups are respectively present in the C2 and C3 positions. In TSr$_{trans}$, these groups are more separated as compared to that in TSr$_{cis}$, as revealed by the C1–C2–C3–O1 dihedral angles (TSr$_{trans}$ −115.6° and TSr$_{cis}$ −70.5°). The steric interaction in TSr$_{cis}$ is clearly higher than that in TSr$_{trans}$. The Coulombic repulsion between the phenyl and lone pairs on nitrogen (N1) can additionally contribute to the energy differences between these TSs. In TSr$_{cis}$, phenyl group is closer to the ylidic nitrogen as compared to that in TSr$_{trans}$ (N1–C2–C3–C4 dihedral is 31.9° in TSr$_{cis}$ while it is −124.5° TSr$_{trans}$). This repulsion leads to considerable widening of C3–C2–N1 and C2–C3–C4 bond angles, which are respectively 106.7° and 119.6° in TSr$_{trans}$ while the corresponding bond angles are 111.9° and 122.5° in TSr$_{cis}$. A likely C–H···π interaction between the *tert*-butyl group of the ester and the phenyl group of benzaldehyde in TSr$_{trans}$ could also be regarded as contributing to the relative energy order.[44] The TS

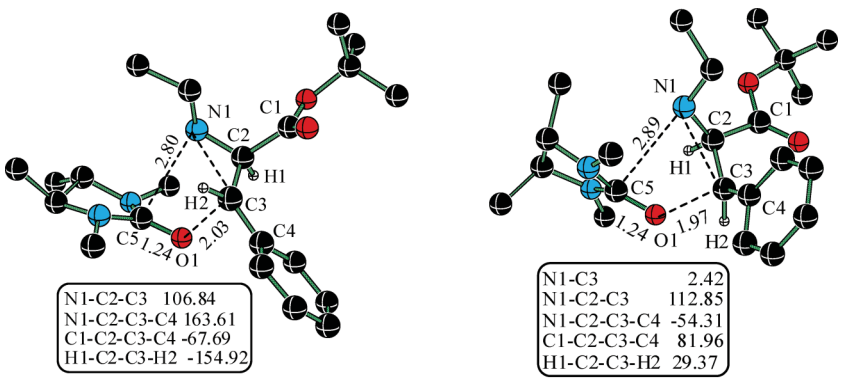

Fig. 3 The mPW1K/6-31G* optimized transition state geometries for the S_Ni like fragmentations of *cis* and *trans* oxa-spirocyclic intermediates.

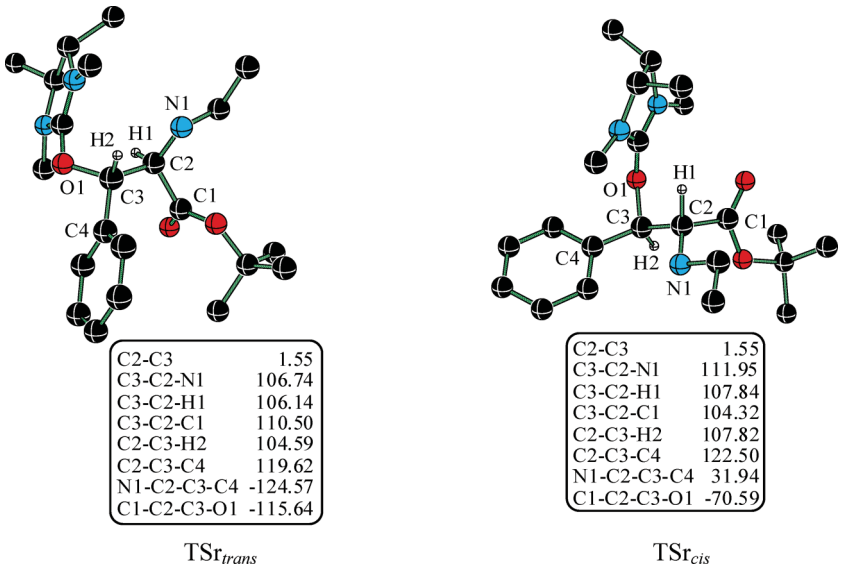

Fig. 4 The mPW1K/6-31G* optimized transition state geometries for the rotation around the C2–C3 bond of *trans* and *cis* 1-oxa-4,6,9-triazaspiro[4.4]nonane intermediates.

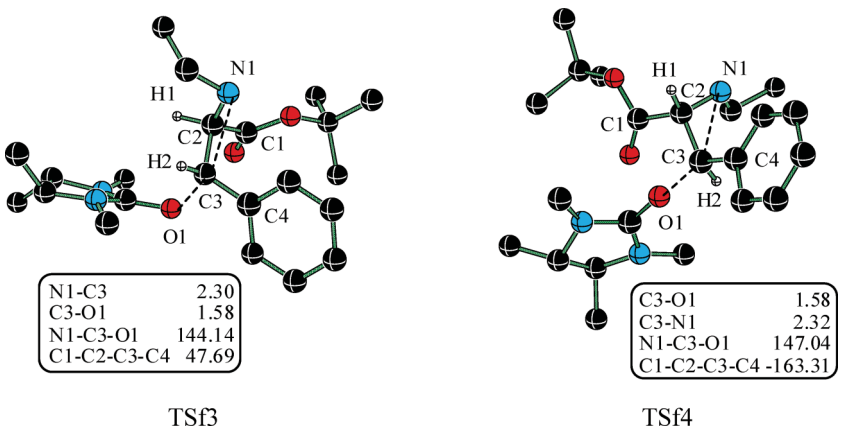

Fig. 5 The mPW1K/6-31G* optimized transition state geometries for the S_N2 like fragmentations of *cis* and *trans* oxa-spirocyclic intermediate.

geometry indicates that similar interactions are not possible in TSr$_{cis}$.

The optimized geometries for the important TSs involved in S_N2 fragmentation mode are provided in Fig. 5. In this step, the anionic N-ethyl group is the internal nucleophile while tetramethylimidazolidinone is the leaving group. Due to the geometric constraints as evident from the optimized geometries, the relative positions of the incoming and the leaving groups do not exhibit a linear trajectory. This can be noticed from N1–C3–O1 angles in both TSf3 and TSf4 which are respectively found to be 144.1° and 147.0°. The relative energy of TSf3 is found to be higher than that of TSf4. Furthermore, the phenyl and *tert*-butyl carboxylic groups in TSf3 are closer, as reflected by the dihedral angle C1–C2–C3–C4 of 47.6° as compared to the −163.3° in TSf4.

Similar to the Hammett analyses of the initial addition step, we have tried to examine how the computed activation energies of the fragmentation step correlate with the nature of the *para* substituent in aromatic aldehydes. The fragmentation steps do not exhibit any good linear correlations. However, the slopes of the Hammett plots for the nucleophilic substitution reactions are found to be negative, indicating that a partial positive charge accumulation is likely in the corresponding TSs.[46] This is consistent with the aforementioned mechanism and the accompanying discussions.

Conclusion

The mechanism and stereoselectivity in aziridine formation between guanidinium ylides and a series of benzaldehydes have been studied using the mPW1K and B3LYP density functional theories. The addition of the *re*-face of the guanidinium ylide on the *re*-face of the aldehyde has been found to be generally the most preferred mode for the initial addition step for both systems bearing electron donating or electron withdrawing substituents at the *para* position of benzaldehyde. Linear Hammett correlations have yielded positive slopes (ρ), suggesting an accumulation of negative charge in the transition states for the addition step. The fragmentation of the ensuing oxaspirocyclic intermediate has been identified to demand higher energy as compared to the addition step. A direct S_Ni route, or a two step process involving ring

opening followed by an S_N2 can lead to aziridine formation. The formation of the *cis* diastereomer could be accounted for by invoking a two step process, consistent with the experimental observations in the case of weakly electron donating/withdrawing substituents. The computed relative energies of key transition states in the case of strong electron donating groups indicate that the S_Ni pathway for the *trans* oxaspirocyclic intermediate could potentially compete with the two step fragmentation route, giving rise to the *trans* diastereomer as the major product. The diminishing energy differences between the S_N2 and ring-opening transition states in the two competitive pathways for strong EWGs indicate that the substituents can steer the diastereoselectivity in favor of *trans*-aziridine. The stereoelectronic effects such as Coulombic interactions due to the nitrogen lone pairs, steric repulsions, and other weak interactions have been identified as responsible for the predicted relative energies between important transition states involved in the mechanistic course. The critical role of the substituent on the guanidinium nitrogen, as noticed in the crucial transition states, could be regarded as a leading hint towards suitable modifications of the chiral catalyst for further exploitation of nitrogen ylide-based chemistry for aziridination reactions.

Acknowledgements

Generous computing time from the IIT Bombay computer center is gratefully acknowledged. R.R acknowledges senior research fellowship from CSIR New Delhi.

References

1 H. M. I. Osborn and J. Sweeney, *Tetrahedron: Asymmetry*, 1997, **8**, 1693. See also ref. 3a and 3b.
2 (*a*) J. B. Sweeney, *Chem. Soc. Rev.*, 2002, **31**, 247; (*b*) V. Buback, M. Mladenovic, B. Engels and T. Schirmeister, *J. Phys. Chem. B*, 2009, **113**, 5282.
3 (*a*) D. Tanner, *Angew. Chem., Int. Ed. Engl.*, 1994, **33**, 599; (*b*) D. Tanner, *Pure Appl. Chem.*, 1993, **65**, 1319; (*c*) H. Ohno, *Chem. Pharm. Bull.*, 2005, **53**, 1211.
4 (*a*) D. Sureshkumar, S. M. Koutha and S. Chandrasekaran, *J. Am. Chem. Soc.*, 2005, **127**, 12760; (*b*) Z.-Q. Liu, Y. Fan, R. Li, B. Zhou and L.-M. Wu, *Tetrahedron Lett.*, 2005, **46**, 1023; (*c*) V. D. Bussolo, M. R. Romano, L. Favero, M. Pineschi and P. Crotti, *J. Org. Chem.*, 2006, **71**, 1696; (*d*) A. B. Smith III and D.-S. Kim, *J. Org. Chem.*, 2006, **71**, 2547; (*e*) V. D. Bussolo, A. Fiasella, L. Favero, F. Bertolini and P. Crotti, *Org. Lett.*, 2009, **11**, 2675.
5 (*a*) P. N. Confalone and E. M. Huie, *J. Org. Chem.*, 1983, **48**, 2994; (*b*) P. N. Confalone and E. M. Huie, *J. Am. Chem. Soc.*, 1984, **106**, 7175; (*c*) R. Grigg, L. M. Duffy, M. J. Dorrity, J. F. Malone, S. Rajviroongit and M. Thornton-Pett, *Tetrahedron*, 1990, **46**, 2213; (*d*) I. Coldham and R. Hufton, *Chem. Rev.*, 2005, **105**, 2765; (*e*) T. M. V. D. Pinho e Melo. Microreview, *Eur. J. Org. Chem.*, 2006, 2873.
6 (*a*) T. Ibuka, *Chem. Soc. Rev.*, 1998, **27**, 145; (*b*) K. Juhl, R. G. Harzell and K. A. Jørgensen, *J. Chem. Soc., Perkin Trans. 1*, 1999, 2293; (*c*) H. Ohno, A. Toda, Y. Takemoto, N. Fujii and T. Ibuka, *J. Chem. Soc., Perkin Trans. 1*, 1999, 2949; (*d*) T. Kubo, S. Sakaguchi and Y. Ishii, *Chem. Commun.*, 2000, 625; (*e*) H. Y. Kim, A. Talukdar and M. Cushman, *Org. Lett.*, 2006, **8**, 1085; (*f*) W. V. Brabandt, Y. Dejaegher, R. V. Landeghem and N. D. Kimpe, *Org. Lett.*, 2006, **8**, 1101; (*g*) D. Sureshkumar, S. Maity and S. Chandrasekaran, *J. Org. Chem.*, 2006, **71**, 1653; (*h*) I. D. G. Watson, L. Yu and A. K. Yudin, *Acc. Chem. Res.*, 2006, **39**, 194.
7 A. A. Cantrill, L. D. Hall, A. N. Jarvis, H. M. I. Osborn, J. Raphyb and J. B. Sweeney, *Chem. Commun.*, 1996, 2631.
8 P. Garner, O. Dogan and S. Pillai, *Tetrahedron Lett.*, 1994, **35**, 1653–1656.
9 (*a*) G. Cardillo, L. Gentilucci, C. Tomasini and M. P. V. Castejon-Bordas, *Tetrahedron: Asymmetry*, 1996, **7**, 755; (*b*) G. Cardillo, L. Gentilucci and A. Tolomelli, *Chem. Commun.*, 1999, 167.
10 D. A. Evans, M. M. Faul, M. T. Bilodeau, B. A. Anderson and D. M. Barnes, *J. Am. Chem. Soc.*, 1993, **115**, 5328.
11 S. K. Kim and E. N. Jacobsen, *Angew. Chem., Int. Ed.*, 2004, **43**, 3952.
12 (*a*) C. J. Sanders, K. M. Gillespie, D. Bell and P. Scott, *J. Am. Chem. Soc.*, 2000, **122**, 7132; (*b*) K. M. Gillespie, C. J. Sanders, P. OShaughnessy, I. Westmoreland, C. P. Thickitt and P. Scott, *J. Org. Chem.*, 2002, **67**, 3450.
13 (*a*) G. Wittig and G. Geissler, *Justus Liebigs Ann. Chem.*, 1953, **580**, 44; (*b*) E. J. Corey and M. Chaykovsky, *J. Am. Chem. Soc.*, 1962, **84**, 867; (*c*) E. J. Corey and M. Chaykovsky, *J. Am. Chem. Soc.*, 1965, **87**, 1353; (*d*) H. J. Cristau, *Chem. Rev.*, 1994, **94**, 1299; (*e*) R. A. Aitken and L. Murray, *J. Org. Chem.*, 2008, **73**, 9781; (*f*) Y. Zhang, Y. K. Liu, T. R. Kang, Z. K. Hu and Y. C. Chen, *J. Am. Chem. Soc.*, 2008, **130**, 2456; (*g*) S. Nakafuji, J. Kobayashi and T. Kawashima, *Angew. Chem., Int. Ed.*, 2008, **47**, 1141; (*h*) S. Redon, S. Leleu, X. Pannecoucke, X. Franck and F. Outurquin, *Tetrahedron*, 2008, **64**, 9293; (*i*) R. Appel, R. Loos and H. Mayr, *J. Am. Chem. Soc.*, 2009, **131**, 704.
14 (*a*) A. H. Li, L. X. Dai and V. K. Aggarwal, *Chem. Rev.*, 1997, **97**, 2341; (*b*) V. K. Aggarwal, J. P. H. Charmant, D. Fuentes, J. N. Harvey, G. Hynd, D. Ohara, W. Picoul, R. Robiette, C. Smith, J. L. Vasse and C. L. Winn, *J. Am. Chem. Soc.*, 2006, **128**, 2105; (*c*) Y. Arroyo, A. Meana, J. F. Rodriguez, M. A. S. Tejedor, I. Alonso and J. L. G. Ruano, *J. Org. Chem.*, 2009, **74**, 4217.
15 (*a*) S. Wilker and G. Erker, *J. Am. Chem. Soc.*, 1995, **117**, 10922; (*b*) H. Takada, P. Metzner and C. Philouze, *Chem. Commun.*, 2001, 2350; (*c*) J. F. Briere, H. Takada and P. Metzner, *Phosphorus, Sulfur Silicon Relat. Elem.*, 2005, **180**, 965.
16 (*a*) B. E. Maryanoff and A. B. Reitz, *Chem. Rev.*, 1989, **89**, 863; (*b*) J. McNulty and K. Keskar, *Tetrahedron Lett.*, 2008, **49**, 7054. See ref. 14.
17 (*a*) F. Amblard, J. H. Cho and R. F. Schinazi, *Chem. Rev.*, 2009, **109**, 4207; (*b*) N. R. Candeias, L. C. Branco, P. M. P. Gois, C. A. M. Afonso and A. F. Trindade, *Chem. Rev.*, 2009, **109**, 2703.
18 G. Pandey, P. Banerjee and S. R. Gadre, *Chem. Rev.*, 2006, **106**, 4484.
19 (*a*) D. Poliakov, A. Rogalyov and I. Shevchenko, *Tetrahedron Lett.*, 2007, **48**, 6798; (*b*) E. P. Urriolabeitia, *Dalton Trans.*, 2008, 5673–5686.
20 (*a*) K. Hada, T. Watanabe, T. Isobe and T. Ishikawa, *J. Am. Chem. Soc.*, 2001, **123**, 7705; (*b*) Y. Tsuchiya, T. Kumamoto and T. Ishikawa, *J. Org. Chem.*, 2004, **69**, 8504; (*c*) W. Disadee and T. Ishikawa, *J. Org. Chem.*, 2005, **70**, 9399; (*d*) T. Haga and T. Ishikawa, *Tetrahedron*, 2005, **61**, 2857.
21 The g-ylide obtained from 2-chloro-1,3-dialkylimidazolinium chloride is typically treated with arylaldehydes in the presence of NaH: T. Isobe, K. Fukuda and T. Ishikawa, *J. Org. Chem.*, 2000, **65**, 7770.
22 (*a*) R. Robiette, *J. Org. Chem.*, 2006, **71**, 2726; (*b*) D. Janardanan and R. B. Sunoj, *J. Org. Chem.*, 2007, **72**, 331; (*c*) D. Janardanan and R. B. Sunoj, *Chem.–Eur. J.*, 2007, **13**, 4805; (*d*) S. A. Stoffregen, R. D. McCulla, R. Wilson, S. Cercone, J. Miller and W. S. Jenks, *J. Org. Chem.*, 2007, **72**, 8235.
23 A good example of computational design of chiral catalyst and subsequent experimental verification of the concept can be seen in (*a*) C. B. Shinisha and R. B. Sunoj, *Org. Biomol. Chem.*, 2007, **5**, 1287; (*b*) D. Janardanan and R. B. Sunoj, *J. Org. Chem.*, 2008, **73**, 8163; (*c*) A. Armstrong, Y. Bhonoah and A. J. P. White, *J. Org. Chem.*, 2009, **74**, 5041.
24 The importance of linear free energy correlations has been identified as a useful indicator of electronic effects in organic reactions since its inception. Select examples include, but not limited to, are (*a*) L. P. Hammett, *J. Am. Chem. Soc.*, 1937, **59**, 96; (*b*) B. Galabov, S. Ilieva and H. F. Schaefer, *J. Org. Chem.*, 2006, **71**, 6382; (*c*) G. O. Jones and K. N. Houk, *J. Org. Chem.*, 2008, **73**, 1333; (*d*) A. Oehlke, A. A. Auer, K. Schreiter, K. Hofmann, F. Riedel and S. Spange, *J. Org. Chem.*, 2009, **74**, 3316; (*e*) S. E. Wheeler and K. N. Houk, *J. Am. Chem. Soc.*, 2009, **131**, 3126; (*f*) E. Clot, C. Megret, O. Eisenstein and R. N. Perutz, *J. Am. Chem. Soc.*, 2009, **131**, 7817.
25 (*a*) D. H. Ess and K. N. Houk, *J. Am. Chem. Soc.*, 2007, **129**, 10646; (*b*) D. H. Ess and K. N. Houk, *J. Am. Chem. Soc.*, 2008, **130**, 10187; (*c*) A. E. Hayden and K. N. Houk, *J. Am. Chem. Soc.*, 2009, **131**, 4084; (*d*) C. B. Shinisha and R. B. Sunoj, *J. Am. Chem. Soc.*, 2010, **132**, 12319.
26 M. J. Frisch *et al. Gaussian 03*, revision C.02; Gaussian Inc.: Wallingford CT, 2004 (see Electronic Supplementary Information for the full citation).

27 B. J. Lynch, P. L. Fast, M. Harris and D. G. Truhlar, *J. Phys. Chem. A*, 2000, **104**, 4811.
28 (*a*) A. D. Becke, *Phys. Rev. A: At., Mol., Opt. Phys.*, 1988, **38**, 3098; (*b*) C. Lee, W. Yang and R. G. Parr, *Phys. Rev. B*, 1988, **37**, 785; (*c*) A. D. Becke, *J. Chem. Phys.*, 1993, **98**, 5648.
29 C. Adamo and V. Barone, *J. Chem. Phys.*, 1998, **108**, 664.
30 (*a*) C. Gonzalez and H. B. Schlegel, *J. Chem. Phys.*, 1989, **90**, 2154; (*b*) C. Gonzalez and H. B. Schlegel, *J. Phys. Chem.*, 1990, **94**, 5523.
31 (*a*) S. Miertus, E. Scrocco and J. Tomasi, *Chem. Phys.*, 1981, **55**, 117; (*b*) B. Mennucci and J. Tomasi, *J. Chem. Phys.*, 1997, **106**, 5151; (*c*) M. Cossi and V. Barone, *J. Chem. Phys.*, 2000, **112**, 2427.
32 The spirocyclic intermediate 1-oxa-4,6,9-triazaspiro[4.4]nonane may also exists in equilibrium with an open chain zwitter ionic intermediate.
33 The *cis* and *trans* notations in the oxa-spirocyclic intermediate refer to the relative dispositions between the phenyl and carboxylic (ester) groups.
34 Relative energies of all diastereomeric TSs for all substituted benzaldehydes exhibited the same trends at the B3LYP and mPW1PW91 levels of theory. The effect of inclusion of diffuse functions in the basis set has also been tested by taking four representative systems. These values, obtained both in the gas-phase and solvent-phase are provided in Tables S1 through S7 in Electronic Supplementary Information. Relative Gibbs free energies obtained at the mPW1K level of theory is summarized in Table S8.
35 Similarly, the values for N1–C2–C3–C4 dihedral angles are respectively 163° and −88°.
36 (*a*) The topological analysis of electron densities are carried out by using Bader's Atom in Molecule formalism as implemented in AIM2000 program; (*b*) R. F. W. Bader, *Atoms in Molecules: A Quantum Theory*, Clarendon Press, Oxford, 1990; (*c*) AIM2000 (Version 2.0), The Buro fur Innovative Software, SBK-Software, Bielefeld, Germany.
37 The correlations between the computed activation barriers and DOPs are provided in Figure S1 in Electronic Supplementary Information. The R^2 values for series $TS1_{re–re}$, $TS2_{re–si}$, $TS3_{si–si}$ and $TS4_{si–re}$ are respectively 0.94, 0.79, 0.95 and 0.95.
38 Deformation energies of both nucleophile and electrophile are provided in Table S9 in Electronic Supplementary Information. Use of deformation energy and the correlation with activation barriers can be seen from the following references. (*a*) A. Diefenbach and F. M. Bickelhaupt, *J. Phys. Chem. A*, 2004, **108**, 8460; (*b*) G. T. de Jong, R. Visser and F. M. Bickelhaupt, *J. Organomet. Chem.*, 2006, **691**, 4341; (*c*) G. T. de Jong and F. M. Bickelhaupt, *ChemPhysChem*, 2007, **8**, 1170; (*d*) G. T. de Jong and F. M. Bickelhaupt, *J. Chem. Theory Comput.*, 2007, **3**, 514; (*e*) I. Fernández, F. M. Bickelhaupt and F. P. Cossío, *Chem.–Eur. J.*, 2009, **15**, 13022.
39 The last geometry, as obtained from the IRC run, is further optimized by using 'opt = calcfc' option, wherein the force constant is evaluated at the same level of theory for the starting geometry. The initial attempts to trace the PRCs have been perfomed at the B3LYP level of theory. The PRCs thus identified by the such methods were subjected to independent geometry optimization at the mPW1K/6-31G* level of theory.
40 J. March *Advanced, organic chemistry* Wiley: New York, 2003, 278.
41 Free energy of activation (in kcal mol^{-1}) for the addition of g-ylide on aryl aldehydes bearing various substituents at the *para* position obtained at the mPW1K/6-31G* level of theory. The details of the model system, where in R = Me, is provided in Table S10 of Electronic Supplementary Information. Hammett plots obtained at the B3LYP/6-31G* level of theory is given in Figure S2 of Electronic Supplementary Information.
42 For Hammett plots for system with R = Me on the g-ylide, see Figure S3 of Electronic Supplementary Information.
43 Interestingly, in the case of EWG, additives such as acetic anhydride and elevated temperatures have been employed. See reference 20d.
44 The topological analysis of electron densities identified the presence of one bond critical point, bcp(ρ) with a value of 0.004, between the phenyl group and one of the interacting hydrogen atom.
45 Calculated *de* and *ee* on the basis of the relative energies of pertinent transition states involved in the most preferred pathway are given in Table S11.
46 Hammett plot for the fragmentation of *cis* and *trans* spiro intermediates of a simplified model obtained at the B3LYP/6-31G* level of theory is given Figure S4 of Electronic Supplementary Information.

